

chip. The device shows a low coupling loss of approximately 1.5 dB per facet, corresponding to 71% fiber-waveguide coupling efficiency.

2. Etchless silicon photonic ring resonators fabrication process flow

The fabrication of the etchless silicon photonic ring resonator is based on a process of selective thermal oxidation of silicon. The etchless silicon waveguides are fabricated from a silicon-on-insulator (SOI) wafer with an initial silicon layer of 500 nm and a buried oxide layer (BOX) of 3 μm . First we grow a thermal oxide layer of 785 nm on the 500 nm SOI which consumes approximately 360 nm of silicon (see Fig. 1(a)). We then pattern the silicon waveguides with electron beam (e-beam) lithography using ma-N 2405 resist (see Fig. 1(b)). Next we etch the patterned thermally grown oxide layer with a RIE tool using fluorine chemistry, leaving behind a thin 50 nm oxide slab throughout the whole wafer (see Fig. 1(c)). This thin oxide slab protects the silicon surface underneath from the ion bombardment and chemical reactions that occur during the plasma etching. After stripping the e-beam resist, we use wet thermal oxidation to selectively oxidize the silicon (see Fig. 1(d)) and define the silicon waveguides with a thin silicon slab (see Fig. 1(e)). Lastly, the waveguides are clad with 300 nm of high temperature oxide (HTO) to give a highly conformal deposition and 1.8 μm of plasma enhanced chemical vapor deposition (PECVD) silicon dioxide to confine the optical mode completely (see Fig. 1(f)).

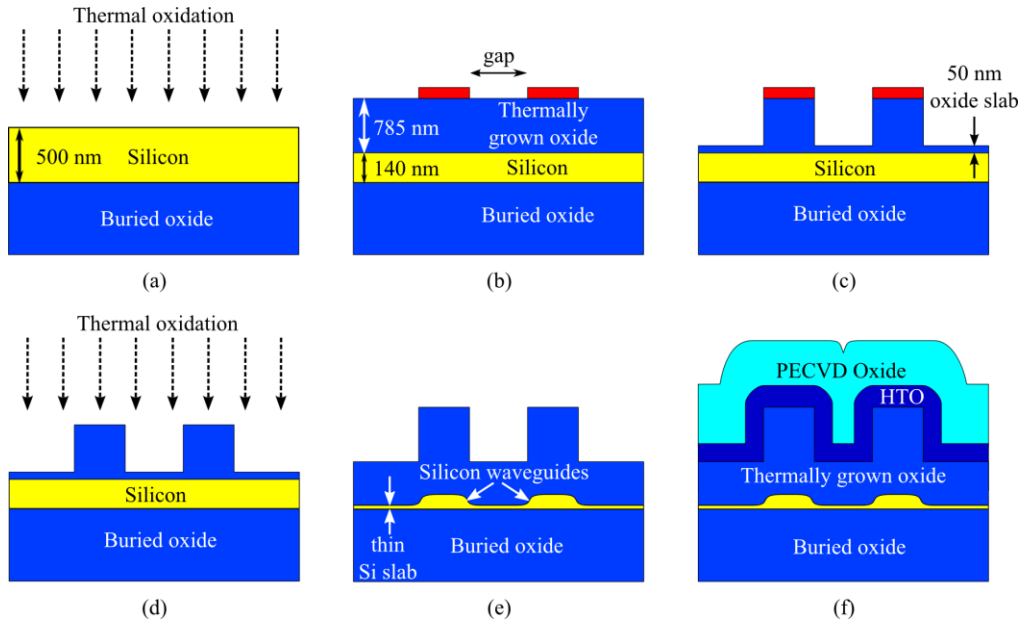


Fig. 1. Etchless silicon photonic ring resonator fabrication process flow. (a) Thermal oxidation of a 500 nm silicon-on-insulator (SOI) to leave behind 140 nm thick silicon layer with 785 nm thick thermally grown oxide on top. (b) Patterning of the waveguides using ma-N 2405 resist, leaving a coupling gap between the ring resonator and bus waveguide. (c) Etching of the thermally grown oxide, leaving behind a thin 50 nm oxide slab. (d) Selective wet thermal oxidation of the silicon. (e) Structural profile of the oxidized silicon waveguides. (f) Deposition of 300 nm HTO and 1.8 μm PECVD silicon dioxide.

3. Etchless silicon photonic ring resonators design

The final structural geometry of an etchless silicon photonic device is dependent on the thickness of the thermally grown oxide layer above the silicon, i.e. the thermal oxidation rate of the silicon at the regions with thin oxide slab is faster than that at the regions with thicker oxide layer. The final structural profile of an etchless silicon waveguide has a slowly varying sidewall which is different from the vertical sidewall of an etched silicon waveguide. In

designing 50 μm -radius etchless silicon photonic ring resonators (see Fig. 2(a)), we use a commercial software Silvaco Athena [27] to simulate the structural profile of the etchless silicon waveguides defined by the selective thermal oxidation process (see Fig. 2(b)). Next we import the simulated profile into Comsol (a finite element modeling software) [28] to compute the modal properties of the etchless silicon waveguides (see Fig. 2(c)). To enable critical coupling at $\lambda = 1.55 \mu\text{m}$, the dimensions of the etchless silicon waveguides following the selective thermal oxidation process are designed to be 800 nm wide by 60 nm tall with a coupling gap of 930 nm [29]. The waveguides are fabricated using 800 nm wide by 785 nm thick etched oxide mask and a coupling gap of 930 nm with a wet thermal oxidation time of 20 minutes (see Fig. 1(d)). The scanning electron microscope (SEM) picture in Fig. 2(d) shows the cross-sectional profile of the coupling region and the structural profile of the fabricated device matches with the simulations accurately. This fabrication technique, which avoids any etching of the silicon layer, results in an ultra-smooth top Si/SiO₂ interface comparable to the interface between the silicon and the buried oxide, as shown in the transmission electron microscope (TEM) picture of the thin oxidized silicon slab (see Fig. 2(e)).

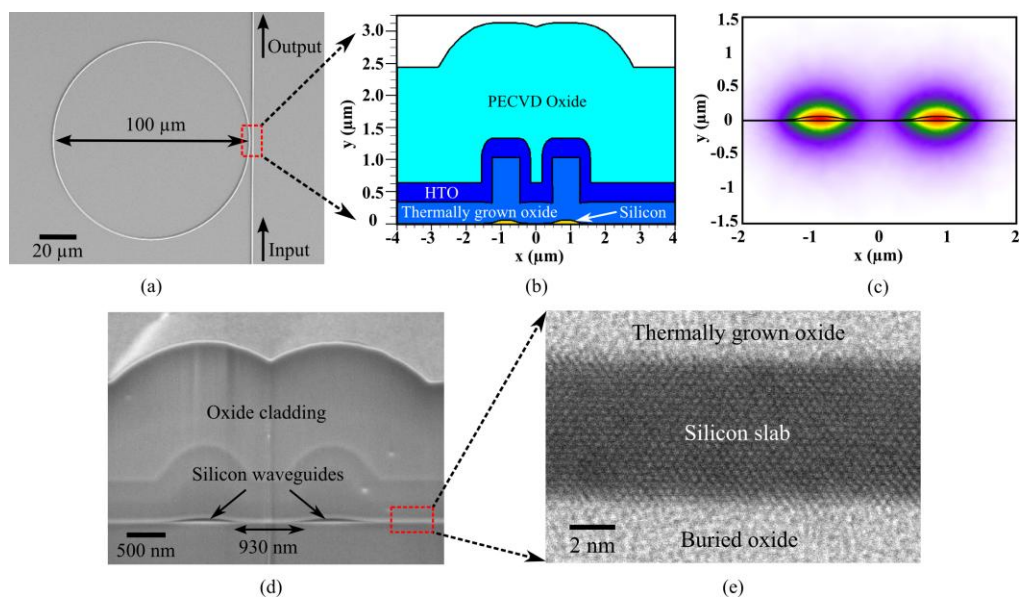


Fig. 2. (a) SEM picture of the fabricated 50 μm -radius etchless silicon photonic ring resonator. (b) Simulated structural profiles of the etchless silicon ring resonator with coupling gap = 930 nm. (c) Symmetric mode of the bus waveguide and the ring resonator. (d) Cross-sectional SEM picture of the coupling region. (e) Transmission electron microscope (TEM) picture of the thin oxidized silicon slab.

The 800 nm wide etchless silicon waveguide forming the ring resonator supports only one mode, i.e. the fundamental TE mode (see Fig. 3(a)). The advantage of supporting only the fundamental TE mode is that the polarization mode conversion is minimized, thus reducing the crosstalk in polarization. The 800 nm waveguide has an effective index of 1.6 at $\lambda = 1.55 \mu\text{m}$ and a mode size of 1 μm wide by 0.52 μm high. On the other hand, a lensed fiber has an effective index of 1.468 and a mode field diameter of 2.5 μm . The coupling of light directly from the lensed fiber into the 800 nm waveguide results in a measured coupling loss of more than 10 dB. This coupling loss is high due to both the refractive index mismatch and mode mismatch between the lensed fiber and the etchless silicon waveguide. To minimize the coupling loss, a 220 nm wide etchless silicon inverse nanotaper with a taper length of 100 μm is integrated at both the input waveguide and output waveguide [30]. The designed inverse nanotaper has an effective index of 1.453 and a mode size of 5 μm wide by 2 μm high (see Fig. 3(b)). Due to this improved match in refractive index and mode size, the coupling loss

from the lensed fiber into the inverse nanotaper is reduced to approximately 1.5 dB. This measured coupling loss is one of the lowest demonstrated in silicon photonic devices.

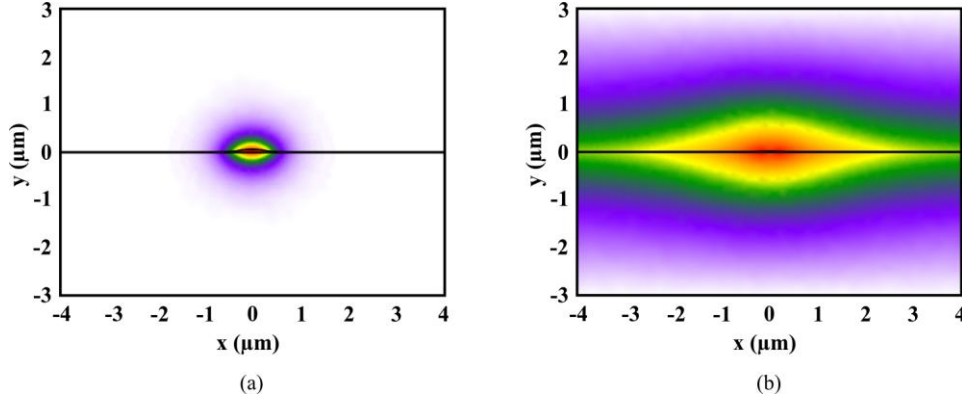


Fig. 3. Transverse electric (TE) mode profile (Ex-component) of (a) Etchless silicon waveguide. (b) Etchless silicon inverse nanotaper.

4. Results and discussions

We demonstrate a high-Q 50 μm -radius etchless silicon ring resonator with an ultra-low total chip insertion loss. We couple a tunable laser light source from a lensed fiber into the etchless silicon inverse nanotaper at the input of the chip through a polarization controller. The light from the output of the chip is then collimated through a lens and collected at a photodetector to measure the total chip insertion loss of TE-polarized light. We observe a clean transmission spectrum, i.e. the Fabry-Perot modulation between the two end facets of the chip is negligible due to the well-designed etchless silicon inverse nanotaper (see Fig. 4(a)).

We measure an ultra-low total chip insertion loss of 2.5 dB from the input lensed fiber to the photodetector at the output. This total chip insertion loss includes the propagation loss of the 1 cm long etchless silicon waveguide and the coupling loss at the chip facets. With a Lorentz fit to the resonance at $\lambda_0 = 1531.416$ nm, we measure the linewidth of the spectrum to be 5.5 pm, giving a loaded quality factor of $Q_{\text{loaded}} \sim 280,000$ (see Fig. 4(b)). The ring is slightly under-coupled at this resonant wavelength. The intrinsic quality factor Q_{int} of the ring can be written as [31]:

$$Q_{\text{int}} = \frac{2Q_{\text{loaded}}}{1 + \sqrt{T_0}}, \quad (1)$$

where T_0 is the fraction of transmitted optical power measured by the photodetector at the resonant wavelength λ_0 . Using Eq. (1), with the measured $T_0 = 0.007$, we calculate the intrinsic quality factor $Q_{\text{int}} = 510,000$.

The total propagation loss per unit length in the ring α_{ring} can be written as [32]:

$$\alpha_{\text{ring}} = \frac{2\pi n_g}{Q_{\text{int}} \lambda_0} = \frac{\lambda_0}{Q_{\text{int}} \times FSR \times R_{\text{ring}}}, \quad (2)$$

where n_g is the group index, FSR is the free spectral range, and R_{ring} is the radius of the ring resonator. Using Eq. (2), with the measured $FSR = 3.25$ nm and $R_{\text{ring}} = 50$ μm , we calculate the ring loss $\alpha_{\text{ring}} = 0.8$ dB/cm. We estimate the coupling loss between the lensed fiber and the etchless silicon inverse nanotaper to be approximately 1.5 dB, corresponding to 71% fiber-waveguide coupling efficiency.

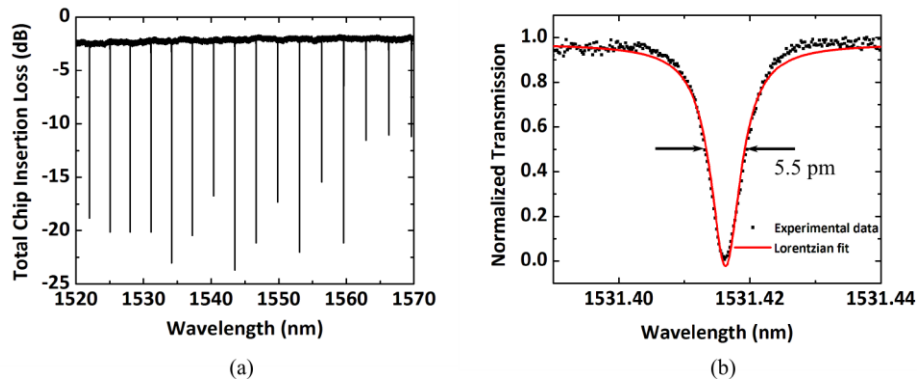


Fig. 4. (a) Through-port transmission spectrum of the ring resonator in transverse electric (TE) polarization. (b) Normalized transmission spectrum at $\lambda_0 = 1531.416$ nm.

5. Conclusion

We designed and fabricated high-Q etchless silicon photonic ring resonators using selective thermal oxidation of silicon without the silicon layer being exposed to any plasma etching throughout the fabrication process. We achieved a high intrinsic quality factor of 510,000 in 50 μm -radius ring resonators, corresponding to a ring loss of 0.8 dB/cm. We also realized an ultra-low total chip insertion loss of 2.5 dB with a fiber-waveguide coupling loss of approximately 1.5 dB by employing etchless silicon inverse nanotapers at both the input and output of the device chip. The low loss etchless silicon photonic ring resonators have promising applications in silicon ring resonators-based optical buffers.

Acknowledgments

The authors acknowledge use of the facilities at the Cornell Center for Materials Research, which is supported by the NSF (award number NSF DMR-0520404), and thank Malcolm Thomas and John Grazul for assistance in operating the focused ion beam and transmission electron microscope. This work was partially funded under the DARPA MTO Si-PhASER project Grant HR0011-09-0013 with the University of California, Davis, and under Grant FA9550-05-1-0414 with Stanford University. This work was performed in part at the Cornell Nanoscale Facility, a member of the National Nanotechnology Infrastructure Network, which is supported by the NSF. Lian-Wee Luo acknowledges a fellowship from Agency of Science, Technology and Research (A*STAR), Singapore.